Electronic Supplementary Material (ESI) for Journal of Materials Chemistry A.

Supporting Information for

Simultaneously Enhancing the Mechanical Robust and Conductivity of Ionogel by *in situ* Formation of Coordination Complexes as Physical Crosslinks

Ning Yu [1], *Yujiang Meng* [1], *Rui Li* [1], *Dongdong Mai* [3], *Shijie Shan* [1], *Xionghui Wu* [1], *Yaling Lin* [2,*], *Anqiang Zhang* [1,*]

1. School of Materials Science and Engineering, South China University of Technology, 381 Wushan Rd., Guangzhou 510641, Guangdong, China
2. College of Materials and Energy, South China Agricultural University, 483 Wushan Rd., Guangzhou 510642, Guangdong, China
3. School of Materials Science and Engineering, Guangdong University of Petrochemical Technology, Maoming 525000, Guangdong, China

* Corresponding author: Prof. Anqiang Zhang (aqzhang@scut.edu.cn), Prof. Yaling Lin (linyaling@scau.edu.cn)

Characterizations of solvent-free coordination ionogel

The NMR spectra were obtained from a Bruker AVANCE III HD 600. The FTIR spectra of the samples were acquired with a Therma Nicolet iS5 spectrometer (Thermo Scientific, USA) with a ZnSe ATR accessory. The TGA curves were measured on a Netzch TG 209 F1. The samples (~10 mg) were heated from 30 °C to 900 °C at a rate of 20 °C/min in a N_2 atmosphere. XRD measurements (D8 Advance, Bruker, Germany) were taken to determine the phase structure and composition of the coordination ionogel, with a 2θ scanning range of 5-60°. Stress–strain curves were measured on a KJ-1067 tensile test machine with a controlled temperature and humidity chamber (Dongguan Kejian Instrument Co. Ltd., China). The measurements were carried out at room temperature at a stretching speed of 100 mm/min. At least three specimens were tested for each ionogel sample, and the average values with standard errors were calculated. The toughness was acquired by integrating the area under the stress–strain curves. DMA (dynamic mechanical thermal spectrometer) (Mettler Toledo Star 1 system) from Mettler Toledo was used to evaluate the dynamic properties. The measurements were carried out in a temperature range of -100 °C to 50 °C with a heating rate of 5 °C/min at a frequency of 1 Hz. Glass temperatures of the $HAIM_{41}$ were measured by a differential scanning calorimeter (DSC 25, TA instruments). The sample with a mass of ≈10 mg was sealed in an aluminum DSC pan and then scanned under a nitrogen atmosphere from -80 °C to 20 °C with a heating rate of 5 °C min^{-1}. Rheological sweeping curves were measured with an Anton Paar MCR 102 rheometer (Austria) equipped with a stainless-steel parallel-plate geometry (diameter: 25 mm). For temperature sweeping tests, a constant frequency of 1 Hz and 1% strain were applied, and the temperature was increased from 20 °C to 160 °C at a heating speed of 2 °C/min. X-ray photoelectron spectroscopy (XPS) of samples was recorded by a Thermo Fisher Scientific ESCALAB 250xi. The energy scanning range was 0-1300 eV, the step size was 1 eV, and analysis was performed using the Avantage software system. Elemental distribution and morphology of the samples were characterized using scanning electron microscope (Merlin, Carl Zeiss Jena, Germany) with an energy dispersive X-ray (EDX) analyzer at 1000× magnification. The sample film was vacuum-dried at room temperature for 24 h and placed on the platform of a contact angle measuring instrument (DSA25, Krüss Company, Germany).

Deionized water was added dropwise onto the film surface using a microsyringe. The shape of the droplet was recorded using a camera and analyzed using software to obtain the contact angle. Transmission electron microscopy (TEM) characterization were carried out on JEM 2100F (JEOL) electron microscope. Ultrathin sections about 200 nm in thickness of the samples were cut by an ultramicrotome Leica EMUC6 under liquid nitrogen atmosphere. To analyze the long-lasting stability of the ionogel, the sample were cut into a spline with a size of 4.5 × 1.5 × 0.01 cm shape and weighed. Then, the ionogel and hydrogel films were put in the constant temperature and humidity chamber (T = 25 °C, relative humidity, RH = 40%), the weight of each sample was measured at regular intervals.

MD simulations methods

Four structures of HAIM-IL-Ni were simulated using the LAMMPS (Large-scale Atomic/Molecular Massively Parallel Simulator) code. The modeling parameters can be found in **Table S2**. A time step of 1 femtosecond was used to ensure system stability and visualize atom vibrations and chemical reactions. Energy minimization was performed using a conjugate gradient algorithm, followed by a relaxation process at 600K for 10 ns under a NVT ensemble to achieve system equilibrium. Data was then collected at 300K using a NPT ensemble for 1 ns. The OPLS-AA force field was employed for all Molecular Dynamics (MD) simulations.

Electrical measurements

The ionic conductivity of the ionogels was measured using an alternating current impedance method on an electrochemical workstation. Specifically, the ionogel was placed between two stainless steel electrodes and secured with a PTFE clip. A sinusoidal voltage amplitude of 0.01 V was applied within a frequency range of 0.01 to 105 Hz. The ionic conductivity was calculated using the formula L/(RA), where L represents the thickness of the tested specimen, R represents the impedance value, and A represents the contact area of the specimen with the electrodes. All samples were tested in triplicate. A two-point probe multimeter (DMM6500, Keithley, USA) was used to measure the real-time resistance of a specimen at different strains. The change in relative resistance was represented as $\Delta R/R_0$, where R_0 is the initial resistance and ΔR is the value of the resistance change. The gauge factor (GF) was determined by calculating the slope of the $\Delta R/R_0$-strain curve through linear fitting.

For the purpose of human motion detection, the sensor was attached to various parts of the volunteers' bodies, and the resistive signal was continuously recorded using a digital multimeter. We have confirmed that informed written consent from all participants was obtained prior to the research.

3D printing of metal coordination ionogel

The 3D models were built using AutoCAD. The precursor solution, $HAIM_{41}$-IL_4-Ni_6, was poured into DLP-based 3D printing equipment (AutoCera, Beijing 10dim Tech. Co., Ltd., China) that utilized a 405 nm projector to print microstructure ionogel flexible sensors. The slurry was stacked and shaped layer by layer as the working stage moved upwards. Each slice layer had a thickness of 100 μm, and the slurry was solidified through UV light irradiation at 405 nm. Once the printing process was completed, the printed $HAIM_{41}$-IL_4-Ni_6 was carefully separated from the retracting stage and rinsed with ethanol for 2 minutes to remove any residual uncured precursor solution. Finally, all printed $HAIM_{41}$-IL_4-Ni_6 samples were stored in a desiccator for future use.

Table S1. Synthesis formula of metal coordination ionogel.

Sample	HA, g	IM, g	IL, (g, wt%HAIM)	$NiCl_2·6H_2O$, (g, wt%HAIM)	[HA]/[IM], mol/mol
$HAIM_{41}$	4.00	0.81	/	/	4/1
$HAIM_{42}$	4.00	1.60	/	/	4/2
$HAIM_{41}$-IL_2	4.00	0.81	0.96 (20 wt%)	/	4/1
$HAIM_{41}$-IL_4	4.00	0.81	1.92 (40 wt%)	/	4/1
$HAIM_{41}$-IL_6	4.00	0.81	2.88 (60 wt%)	/	4/1
$HAIM_{41}$-IL_2-Ni_6	4.00	0.81	0.96 (20wt%)	0.29 (6 wt%)	4/1
$HAIM_{41}$-IL_4-Ni_6	4.00	0.81	1.92 (40 wt%)	0.29 (6 wt%)	4/1
$HAIM_{41}$-IL_6-Ni_6	4.00	0.81	2.88 (60wt%)	0.29 (6 wt%)	4/1
$HAIM_{41}$-IL_4-Ni_2	4.00	0.81	1.92 (40 wt%)	0.09 (2 wt%)	4/1
$HAIM_{41}$-IL_4-Ni_6	4.00	0.81	1.92 (40wt%)	0.29 (6 wt%)	4/1
$HAIM_{41}$-IL_4-Ni_{10}	4.00	0.81	1.92 (40 wt%)	0.48 (10 wt%)	4/1

Table S2. Number of different molecules in the simulation system.

Sample	Number of HAIM	Number of IL	Number of $NiCl_2 \cdot 6H_2O$
$HAIM_{41}$	800	/	/
$HAIM_{41}$-IL_4	800	500	/
$HAIM_{41}$-IL_4-Ni_2	800	500	20
$HAIM_{41}$-IL_4-Ni_6	800	500	60

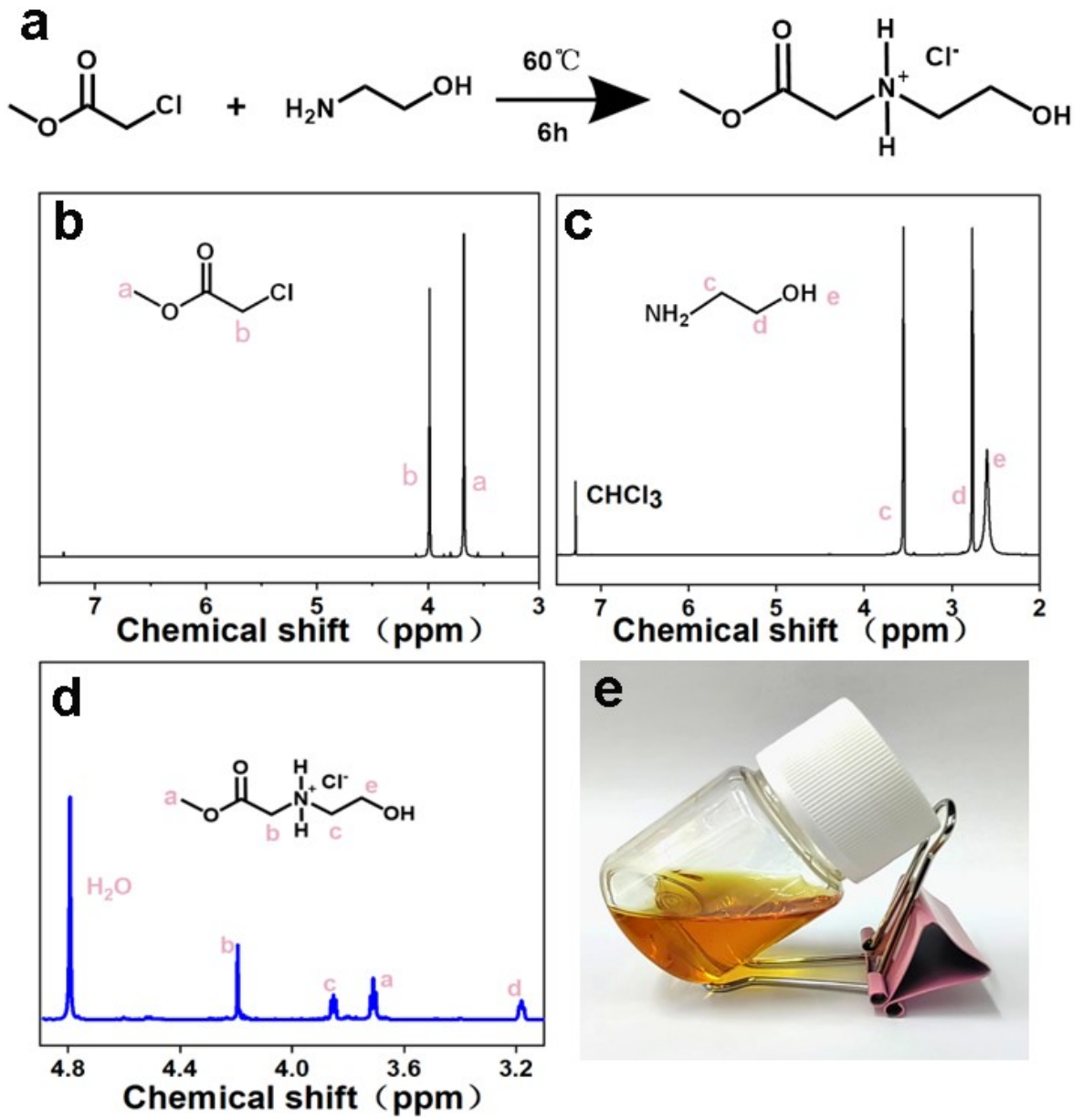

Figure S1. (a) The synthesis process of IL. ^1H NMR spectra of (b) 2-aminoethanol (in $CDCl_3$), (c) methyl chloroacetate (in $CDCl_3$) and (d) IL (in D_2O). (e) Digital photos of IL at room temperature.

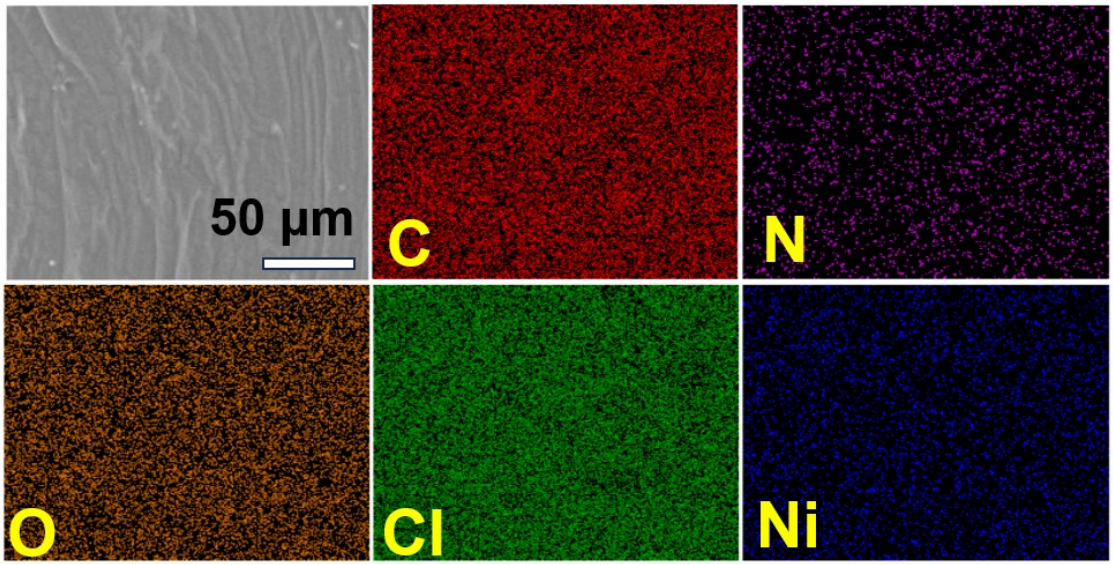

Figure S2. (a) EDS image of $HAIM_{41}$-IL_4-Ni_6 section.

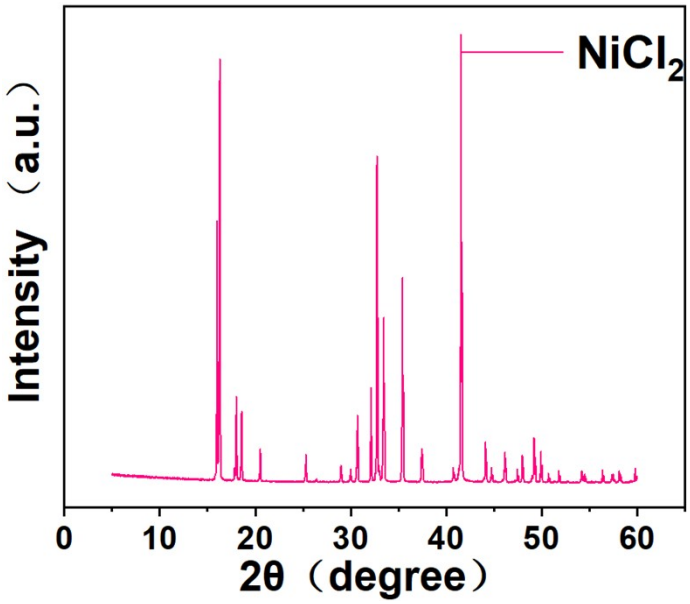

Figure S3. The XRD of $NiCl_2 \cdot 6H_2O$

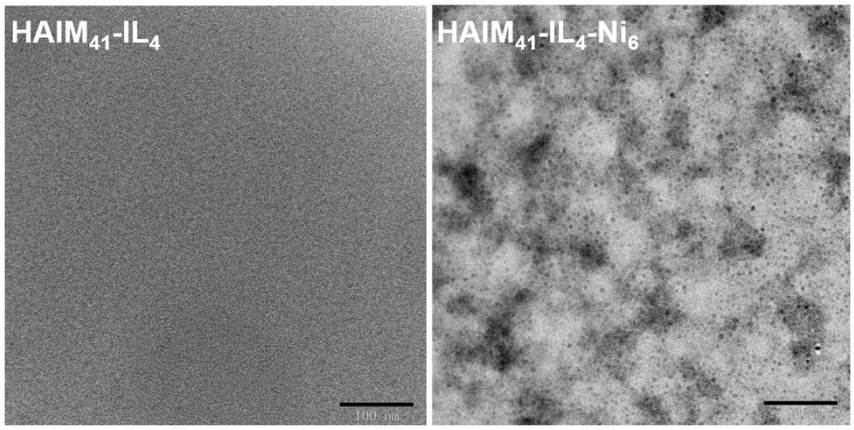

Figure S4. TEM of $HAIM_{41}$-IL_4 and $HAIM_{41}$-IL_4-Ni_6.

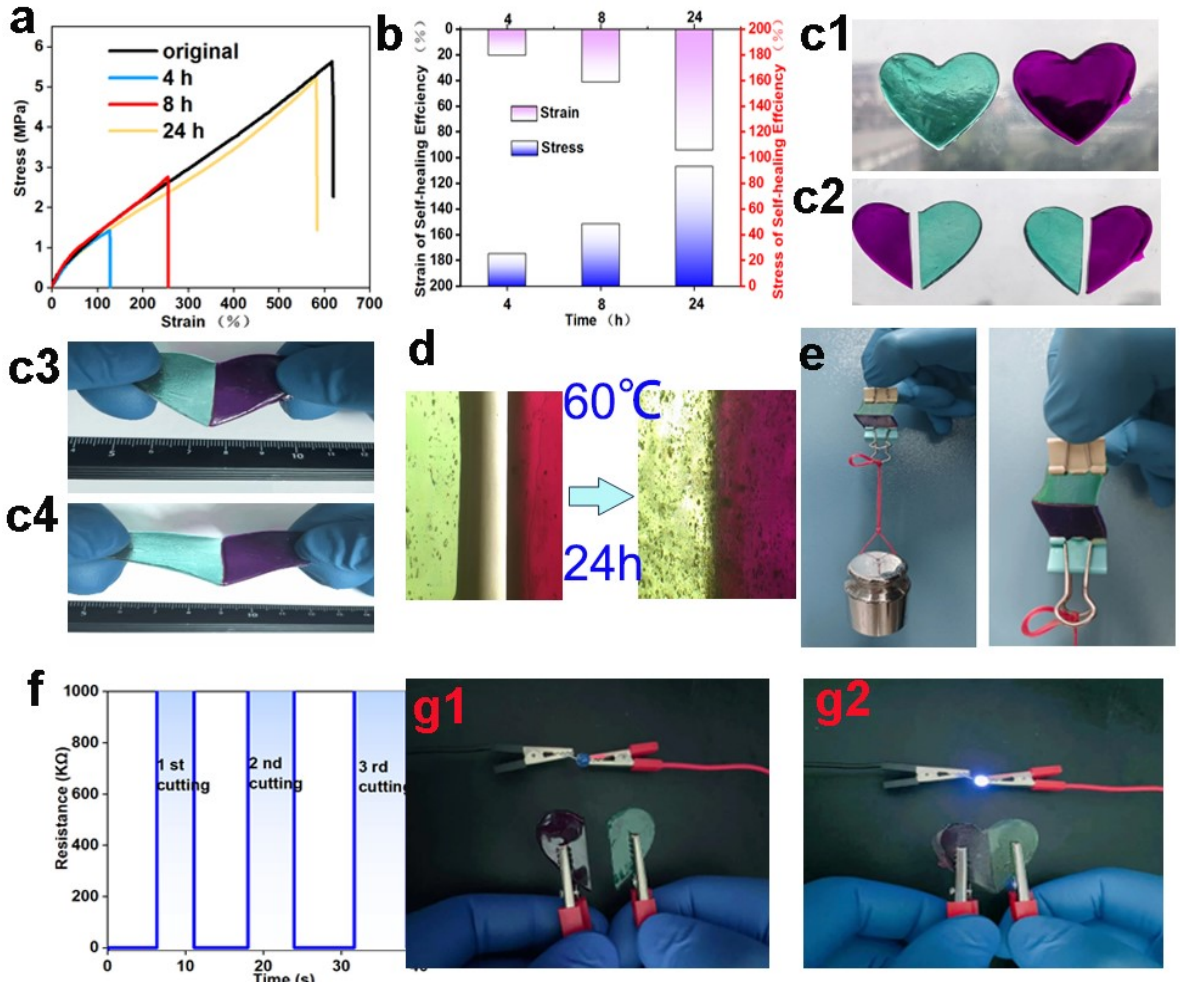

Figure S5. Self-healing of the $HAIM_{41}$-IL_4-Ni_6: (a) the stress-strain curves of $HAIM_{41}$-IL_4-Ni_6 before cut and after healing for different periods of time. (b) The self-healing efficiencies calculated by the tensile strength of original and healed samples. (c) The self-healing process with original and dyed heart-shaped $HAIM_{41}$-IL_4-Ni_6 sample. (d) The microscopic observation of self-healing process. (e) The healed sample can

be lifted with a 500g weight. (f) Resistance changes of $HAIM_{41}$-IL_4-Ni_6 during the cutting and contacting process. (g) The change in LED brightness during the cutting and contacting process.

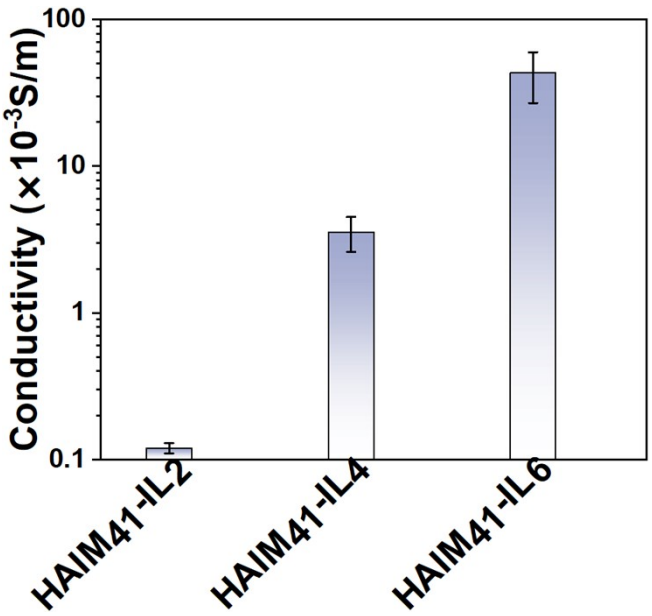

Figure S6. Ionic conductivity of ionogel with different IL content.

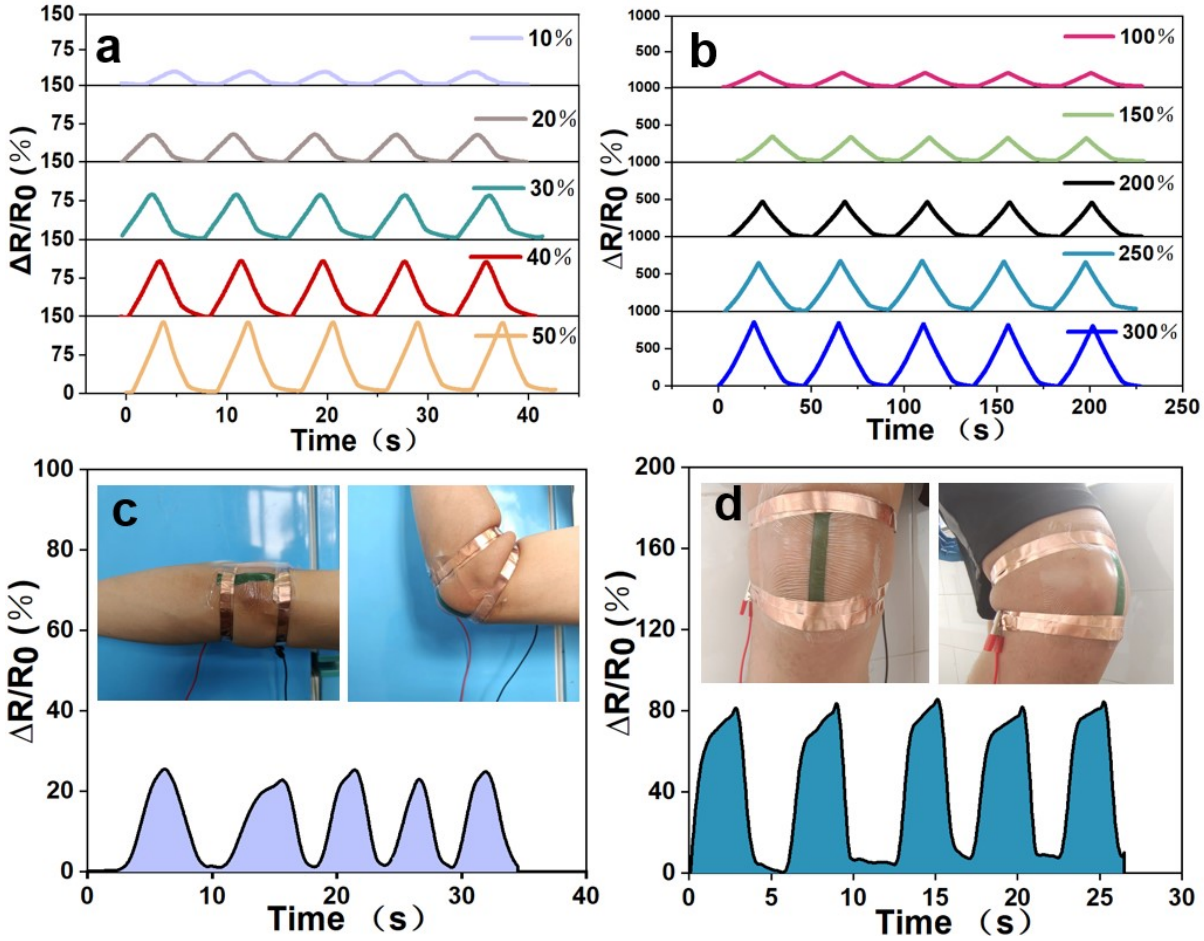

Figure S7. (a) Cyclic tensile tests at small strains (10%~50%) and (b) large strains (100%~300%). Response of the resistance signals of the sensor to detect (c) elbow bending and (d) knee bending.

Figure S8. Assemble $HAIM_{41}$-IL_4-Ni_6 into a writing pen and **writing** "SCUT", "福 (fu)"and "heart-shaped".

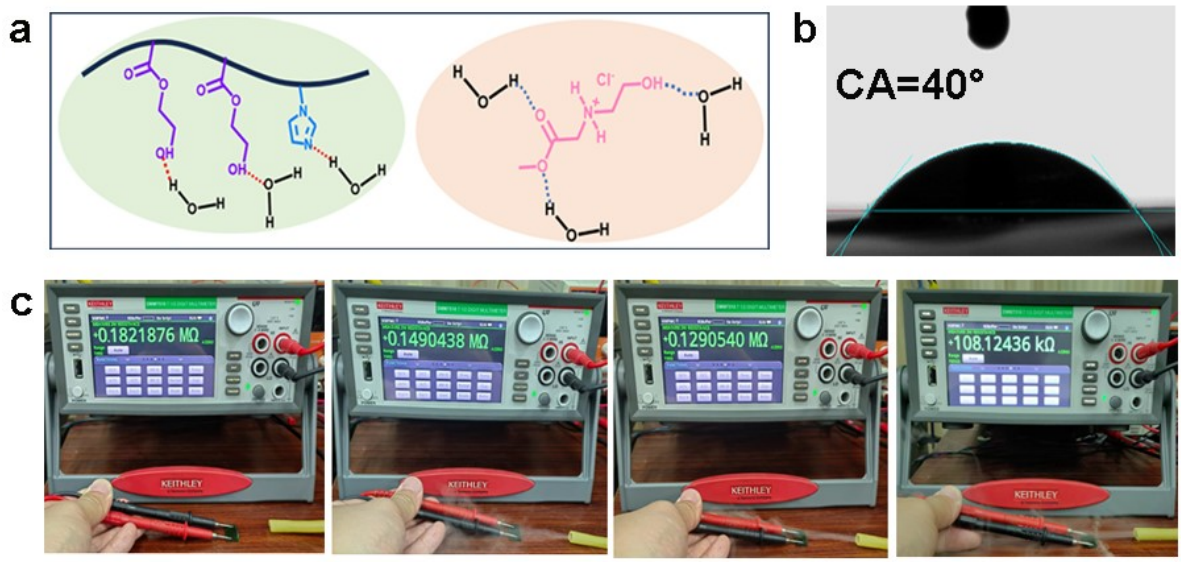

Figure S9. Humidity-sensing mechanism of the $HAIM_{41}$-IL_4-Ni_6. (b) Contact angle of $HAIM_{41}$-IL_4-Ni_6. (c) The resistance of $HAIM_{41}$-IL_4-Ni_6 decreases with changes in humidity.

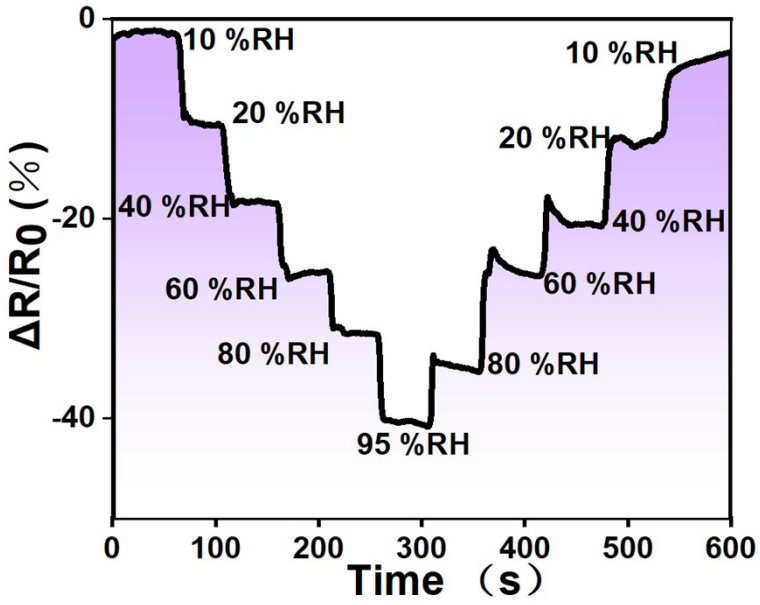

Figure S10. Recovery curves of different $HAIM_{41}$-IL_4-Ni_6 at different RH levels.

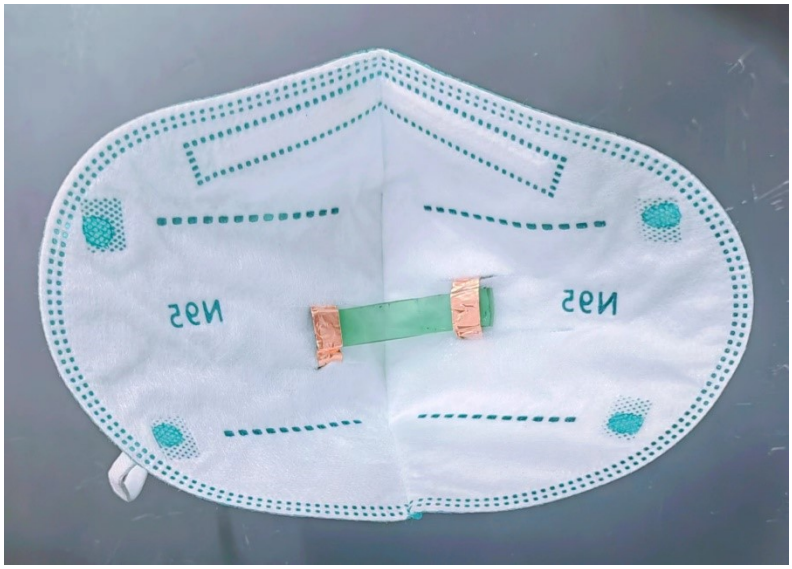

Figure S11. Assemble $HAIM_{41}$-IL_4-Ni_6 **onto a medical mask**

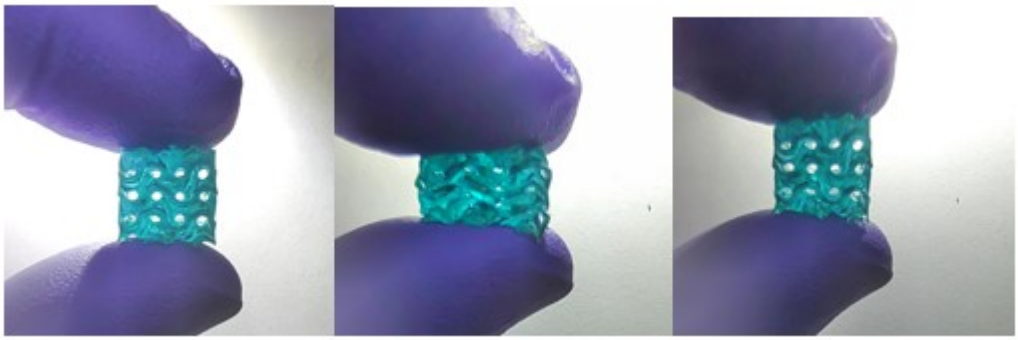

Figure S12. Porous structure's deformation under loading and unloading.

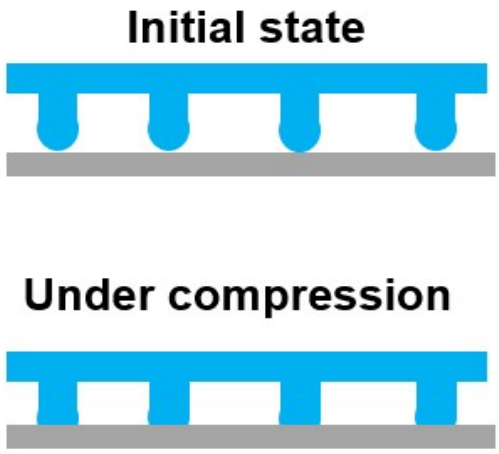

Figure S13. Schematic of a printed ionogel array with hemisphere on the surface

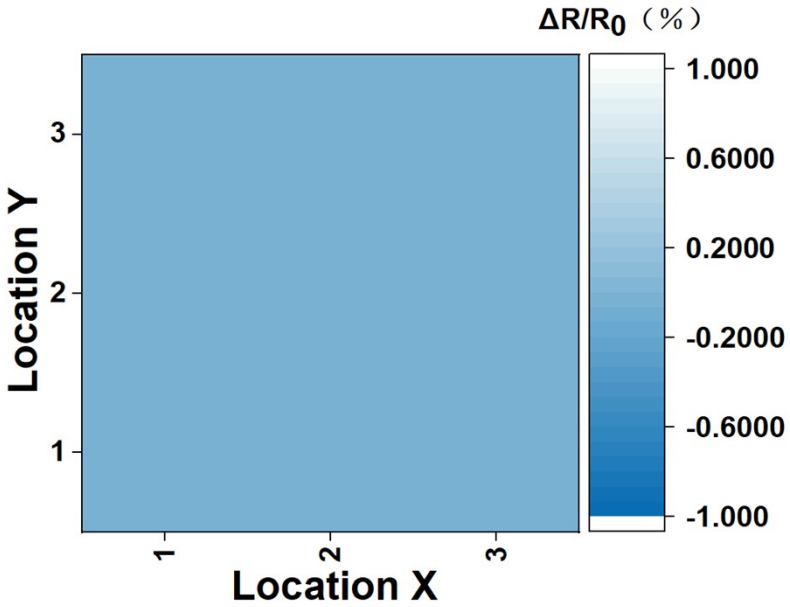

Figure S14. 2D mapping image of sensor without applying pressure.